

Poly(ether ether ketone)/wrapped graphite nanosheets with poly(ether sulfone) composites: Preparation, mechanical properties, and tribological behavior

Wenlong Jiang,¹ Xu Jin,² Haibo Zhang,¹ Bo Jiang,¹ Zhenhua Jiang,¹ Yunhe Zhang¹

¹Alan G. MacDiarmid Laboratory, College of Chemistry, Jilin University, Changchun, 130012, People's Republic of China

²Research Institute of Petroleum Exploration and Development, Petrochina, Beijing 100083, People's Republic of China

Correspondence to: Y. Zhang (E-mail: zhangyunhe@jlu.edu.cn)

ABSTRACT: Antiwear composites with extraordinary tribological performances and good mechanical/thermal properties were developed by the dispersion of poly(ether sulfone) (PES) wrapped graphite nanosheets (GNSs) inside a poly(ether ether ketone) (PEEK) matrix via melt blending. The tribological behaviors and the mechanical/thermal properties of the composites were carefully investigated. Compared with pure PEEK and PEEK/GNS composites, the PEEK/wrapped GNS composites exhibited considerable enhancements in those performances; these were attributed to the eliminated layer of PES; this elimination not only eliminated the GNS aggregation inside the PEEK matrix for homogeneous distribution inside the PEEK matrix but also enhanced the interfacial adhesion between the PEEK and wrapped GNSs. © 2014 Wiley Periodicals, Inc. *J. Appl. Polym. Sci.* **2015**, *132*, 41728.

KEYWORDS: friction; mechanical properties; thermal properties; wear and lubrication

Received 20 May 2014; accepted 3 November 2014

DOI: 10.1002/app.41728

INTRODUCTION

Poly(ether ether ketone) (PEEK) has been widely studied in the aeronautic, automotive, and electric industries; this study has been driven by its excellent mechanical properties, thermal stability, good chemical resistance, and high wear resistance.^{1–4} However, in its neat form, PEEK always exhibits a high friction coefficient ($\mu \geq 0.4$) in dry sliding;^{5–8} this hinders its utilization in tribological systems. Current interest lies in how to enhance the tribological performance of PEEK composites to extend its applications in both academic and industrial fields.

Graphite nanosheets (GNSs), as excellent solid lubricants, have been extensively used in tribological systems based on GNS-filled polymer composites because of their unique mechanical and thermal properties.^{9–12} One mechanism of the reduction in the friction coefficient is the formation of a transfer film on the counterface.¹³ The transfer film can reduce the friction coefficient and wear rate by preventing direct contact between the sample and the counterface. However, GNSs suffer severe aggregation because of their strong p–p stacking tendency and high cohesive energy; this reduces the homogeneity of GNS-filled polymer composites.

Poly(ether sulfone) (PES), which possesses a high glass transition, high thermal stability, and high impact strength, is an engineering thermoplastic.^{14–20} Additionally, the aromatic struc-

ture of PES can generate strong interactions with GNSs to eliminate GNS aggregation. Furthermore, PES also has good compatibility with PEEK. These outstanding performances make PES a good candidate as an intermediate layer for GNS-filled PEEK. In this study, PES/wrapped GNS composites were prepared by the dispersion of PES/wrapped GNSs inside a PEEK matrix via melt blending. In contrast to those found for PEEK and PEEK/GNS composites, enhanced tribological and mechanical/thermal properties were successfully obtained.

EXPERIMENTAL

Materials

PEEK and PES were supplied in powder form by Changchun Jilin University Super Engineering Plastics Research Co., Ltd. (People's Republic of China). The melt flow index of PEEK was 26 g/10 min, and the inherent viscosity of PES was 0.34 dL/g. GNSs were purchased from Xiamen Knano Graphene Technology Co., Ltd. *N,N*-Dimethylformamide, *N,N*-dimethylacetamide (DMAc), and ethanol were obtained from commercial sources and were used as received.

Preparation of the Wrapped GNSs

First, a quantity of PES powder was dissolved in DMAc to obtain a solution. Subsequently, GNSs were added to the solution under slow stirring conditions. Lastly, this DMAc solution containing GNSs was stirred for 1 h at 50°C, after which it was

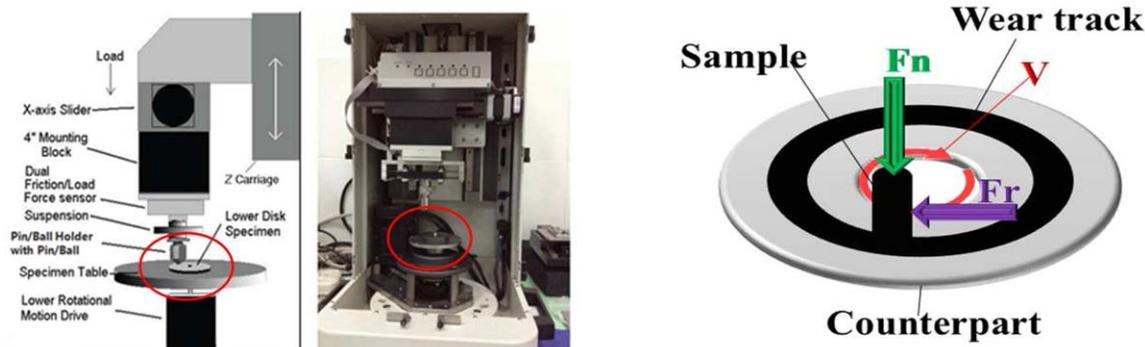


Figure 1. Schematic diagram of the P-o-D test apparatus (left) and schematics of the P-o-D tribological tests (right). [Color figure can be viewed in the online issue, which is available at wileyonlinelibrary.com.]

poured into deionized water. The precipitate came into being and was collected by filtration. The product was washed with deionized water several times to remove DMAc and obtain the wrapped GNSs.

Preparation of the Composite

The PEEK and wrapped GNSs were first premixed with a high-speed mixer. The predispersion mixture was further blended with a Haake PTW16/25p corotating twin-screw extruder at a screw speed of 100 rpm. The temperature profile of the barrel was 320/330/350/350/350/340°C from the hopper to the die. The weight fractions of the wrapped GNSs in the composites were 2, 5, 10, and 20 wt %. The obtained samples were cut into granules, dried at 120°C for 4 h, and molded by an injection-molding machine for the different measurements. The PEEK/GNSs were prepared by the same procedure used for the PEEK/wrapped GNSs.

Characterization. X-ray diffraction (XRD) was carried out with a Rigaku D/Max-2500 X-ray apparatus. The morphologies of the GNSs and wrapped GNSs were characterized with transmission electron microscopy (TEM; JEOL JEM-1200EX) at an accelerating voltage of 200 kV. To investigate the morphologies of the GNSs and wrapped GNSs, the samples were dispersed in dimethylformamide by ultrasonication, and some pieces were collected on carbon-coated copper grids for observation. The fractured surfaces and polished cross sections of the pure PEEK and its composites were analyzed with a Shimadzu SSX-550 Superscan scanning electron microscope after a gold layer was sputtered on their surfaces. The thermogravimetric analyses (TGA) were determined in a nitrogen atmosphere with a heating ramp of 10°C/min, and the samples were contained within open aluminum pans on a PerkinElmer TGA-7. Tensile and three-point flexural tests were performed with a Shimadzu AG-1 testing machine at room temperature. The rates of the tensile and flexural tests were 5 and 2 mm/min, respectively.

Tribological experiments were performed with a UMT-2 pin-on-disc (P-o-D) apparatus (Figure 1) according to the standard ASTM G 99-04. The wear pins were molded by an injection-molding machine with dimensions of diameter (Φ) = 6.3×18.8 mm². The composite specimens were rotated against a 45# Cr6 steel ring with a diameter of 20 mm for 60 min under dry conditions at room temperature. The apparent pressure was 1 MPa, and the sliding velocity was 1.0 m/s. The contact surfaces of the composite block

and the carbon steel ring were preworn with 900# grinding paper and washed with acetone. We calculated the mass loss of the specimens after the frictional test (Δm) by subtracting its initial weight by its final weight after the sliding, and we calculated the specific wear rate (W_s) of the material using the following equation:

$$W_s = \frac{\Delta m}{\rho FL} \text{ (mm}^3\text{/Nm)}$$

where ρ is the density of the specimen, F the normal load applied on the specimen during sliding, and L is the total sliding distance.

RESULTS AND DISCUSSION

Characteristics of the GNSs and Wrapped GNSs

Typical TEM images of the GNSs and wrapped GNSs are shown in Figure 2. These indicated that the GNSs existed in the form of a thin film with a few ripples within the plane. After surface modification, distinctive morphological changes were observed, as shown in Figure 2(b), in which a rougher surface could be detected. In addition, we found that the surface modification had no effect on the diameter of the GNSs, and the size still ranged from 2 to 4 μ m.

The XRD patterns were used to characterize the GNSs and wrapped GNSs, as shown in Figure 3. For the GNSs and wrapped GNSs, a characteristic peak of $2\theta = 26.5^\circ$, corresponding to the (002) diffraction, was clearly detected. With Bragg's law and Scherer's equation, the distance between the adjacent graphenes (d), composed of the graphite, and also the size of the crystal (C) were determined. Table I shows that the surface modification did not increase the distance between the graphenes. Moreover, we found that the crystal size was different between the GNSs and wrapped GNSs. The GNSs presented a larger crystal; this indicated a higher stacking of graphenes.²¹

Preparation and Morphologies of the Composites

PEEK/GNS and PEEK/wrapped GNS composites were successfully fabricated by melt-blending technology and analyzed by XRD, as shown in Figure 3. In the XRD, both composites showed that the peak at $2\theta = 26.5^\circ$ was still present; this meant that the GNSs still existed in the aggregating form.²² Nevertheless, the peak in the PEEK/GNS composites was weaker than that in the PEEK/wrapped GNS composites; this implied a

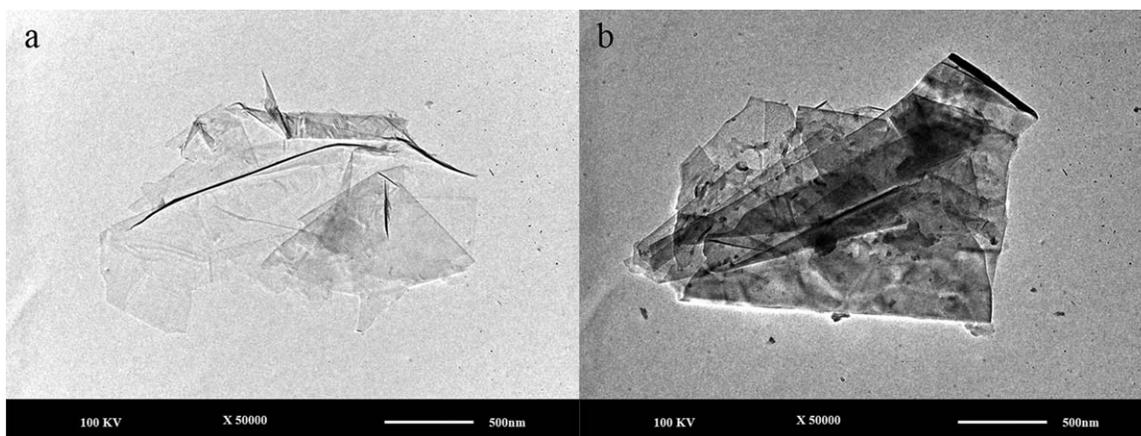


Figure 2. TEM micrographs of the (a) GNSs and (b) wrapped GNSs.

more even distribution of GNSs in the PEEK/wrapped GNS composites.

To directly display the GNS dispersion in the PEEK/GNS and PEEK/wrapped GNS composites, scanning electron microscopy was used to characterize the cross sections after tensile testing. Without the intermediate layer, the GNSs were aggregated and formed bundles inside the PEEK matrix [Figure 4(a,b)]; this was the same as listed in previous reports.^{23,24} As PES was introduced into the system, the GNS dispersion was greatly improved, as shown in Figure 4(c), with a PES/GNS proportion of 10 wt %. This confirmed the excellent interfacial compatibility between the PEEK matrix and PES. When the PES/GNS proportion reached 20 wt % [Figure 4(d)], some aggregations of PES/GNS inside the PEEK matrix could be detected.

Mechanical Properties of the Composites

The tensile strength, elongation at break, and flexural strength values of both the PEEK/GNS composites and PEEK/wrapped GNS composites at different loading levels (from 0 to 20 wt

%) are shown in Figure 5; this figure shows that the enhanced tensile strength, elongation at break, and flexural strength of the PEEK/wrapped GNS composites were better than those of the PEEK/GNS composites. Additionally, we also found that the tensile and flexural strength of the two types of composites first rose and then decreased when the filler content increased. Meanwhile, the elongation at break decreased. In particular, the tensile strength for the two types of composites showed a maximum peak, which occurred at a GNS or wrapped GNS content of 10 wt %, as depicted in Figure 5(a). This was attributed to the counterbalance of the increased surface fracture energy and the increased sizes of the voids as the filler content in the polymer composites increased.^{25,26} It has been generally accepted that dispersed fillers inside composites can make the crack propagation path longer, absorb a portion of the energy, and enhance the plastic deformation. Thus, both the surface fracture energy of the materials and the strength of the composites increased.²⁵ However, a further increase in the filler content increased the size of the voids for the detachment of PEEK from the filler, and this initiated the main crack.²⁵ In addition, the inevitably increased aggregation of dispersed fillers led to a decreased mechanical strength.²⁴

Thermal Properties of the Composites

Figure 6 shows the TGA curves of the pure PEEK and its composites filled by GNSs or wrapped GNSs. All of the samples possessed outstanding thermal stabilities, with a 5% weight loss decomposition temperature above 570°C. Moreover, we clearly detected that the incorporation of GNSs significantly improved the thermal stability of the PEEK polymer. It is notable that the TGA data for the PEEK/wrapped GNS

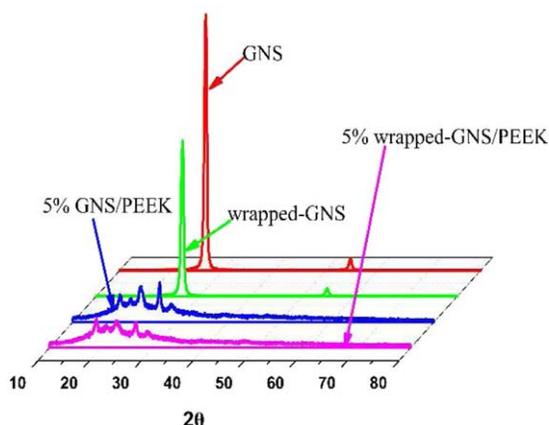


Figure 3. XRD of the GNSs, wrapped GNSs and 5% GNS/PEEK and 5% wrapped GNS/PEEK composites. [Color figure can be viewed in the online issue, which is available at wileyonlinelibrary.com.]

Table I. Distances Between the Graphite Layers and the Crystal Sizes of the GNSs and Wrapped GNSs

| Sample | <i>d</i> (nm) | <i>C</i> (nm) |
|--------------|---------------|---------------|
| GNSs | 0.3431 | 15.71 |
| Wrapped GNSs | 0.3426 | 14.19 |

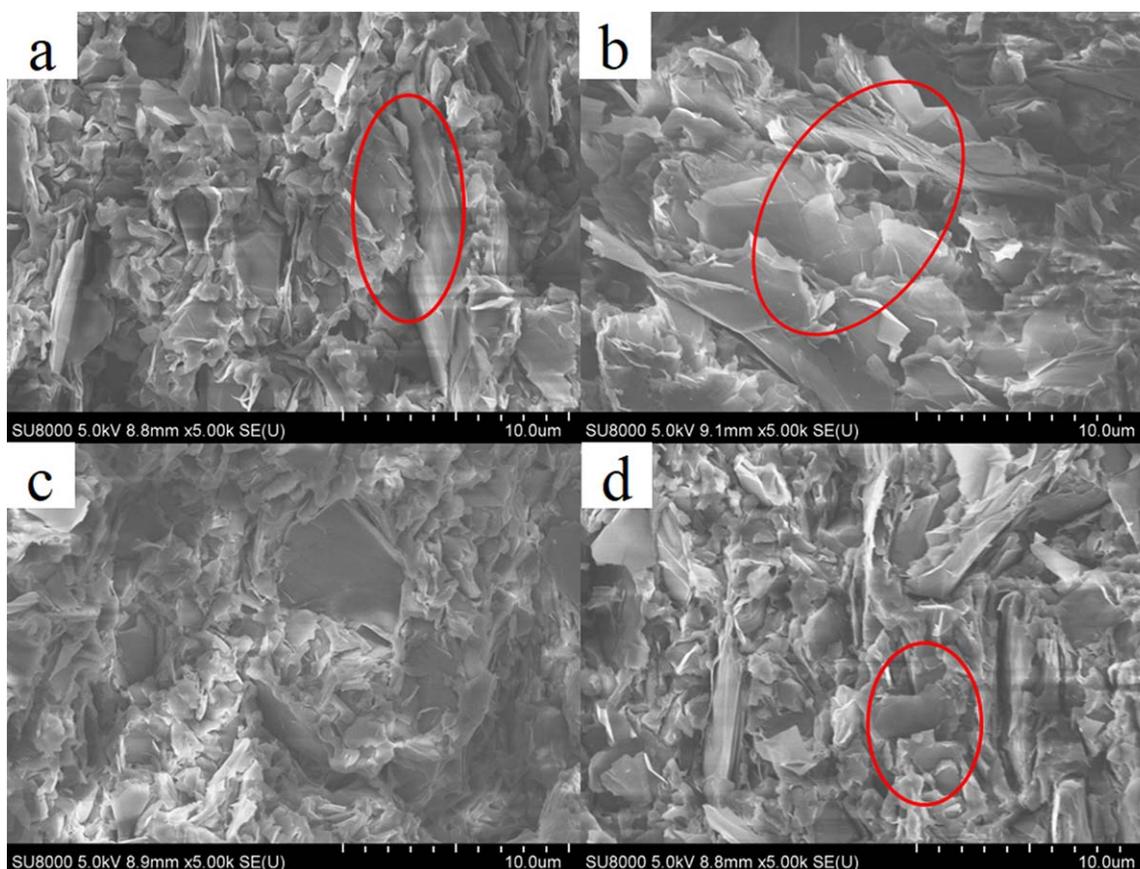


Figure 4. Typical scanning electron micrographs of the fractured surfaces of the PEEK composites in liquid nitrogen: (a) PEEK/GNS = 90/10, (b) PEEK/GNS = 80/20, (c) PEEK/wrapped GNS = 90/10, and (d) PEEK/wrapped GNS = 80/20. [Color figure can be viewed in the online issue, which is available at wileyonlinelibrary.com.]

composites were peculiarly striking: when the wrapped GNS proportions reached 20 wt %, an unprecedented enhancement of the thermal stability of nearly 29°C appeared with a 5% weight loss. This indicated that the wrapped GNSs effectively restricted the thermal motion of the PEEK chains and enhanced the thermal stability.

Tribological Behaviors of the Composites

The friction coefficients and wear rates are the primary metrics of performance in tribological systems. The *friction coefficient* is defined as the ratio of the force that resists sliding to the normal force, and the *wear rate* is defined as the volume of material removed per unit of normal load per unit distance of sliding. A low friction coefficient and wear rate are the most important characteristics of the antiwear material.

Figure 7 shows that the curves of the friction coefficients of PEEK and the composites varied with the sliding time at 1 m/s under a 1-MPa applied load. For all of the materials, in the sliding stage, the friction coefficient increased remarkably at the beginning and fluctuated slightly at the steady stage. This phenomenon could be explained as follows: at the beginning of the sliding stage, the PEEK matrix and GNSs were likely to be worn out from the composite pin because of the plowing from the counterface; they became the third-body abrasive, and this caused high friction.²⁷

When the friction time increased, the counterface was abraded, and the transfer film was formed; this resulted in a stable friction process. We also detected that the friction coefficients of those two GNS-based composites were all lower than that of pure PEEK; this confirmed that the GNS fillers reduced the friction coefficient of the PEEK polymer.

To further investigate the influence of the filler loading amount on the tribological behavior of the composites, the friction coefficient and wear rate of the composites versus the contents of the fillers were measured, as shown in Figure 8. When the filler or wrapped filler content in the composites was increased, the friction coefficients of the two types of composites showed similar tendencies: they first decreased and then increased with a minimum value at a weight ratio of about 10 wt % for the dispersion state of the GNSs. With the addition of the GNSs, plenty of the GNSs spread symmetrically on the sliding surface to reduce the direct contact between the steel counterpart and the composites; this decreased the friction coefficient. With a continuous increase in GNSs, a large amount of GNSs might have agglomerated, as shown in Figure 4(b,d); this deteriorated the coefficient of friction.²⁸ Figure 8(b) shows that the wear rates of all of the kinds of composites were higher than that of pure PEEK. This directly confirmed that the presence of the GNS fillers promoted the spalling of the PEEK, and the PEEK debris caused abrasive wear.

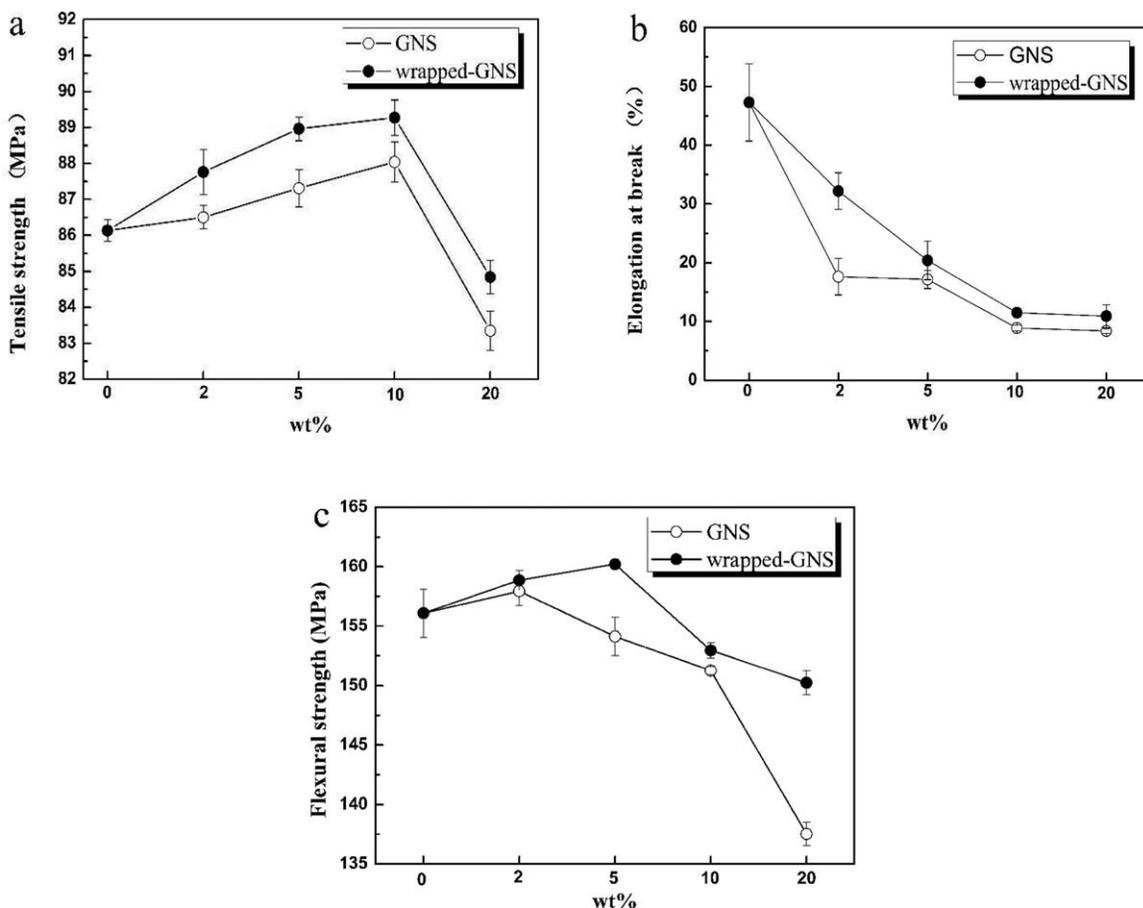


Figure 5. (a) Tensile strength, (b) elongation at break, and (c) flexural strength values of PEEK and its composites.

It is generally recognized that the most common types of wear of polymers are abrasion, adhesion, and fatigue. Figure 9(a,b) shows, with low and high magnifications, respectively, the worn surface of the PEEK produced under the conditions of an applied load of 1 MPa and a sliding velocity of 1 m/s.

The corresponding surface was very rough, with slight plowing and a little tiny debris suggesting that both the abrasive wear and adhesive wear constituted the main wear mechanism. Figure 9(c,d) shows the worn surface of the PEEK/GNS composites. Compared with pure PEEK, the surface of

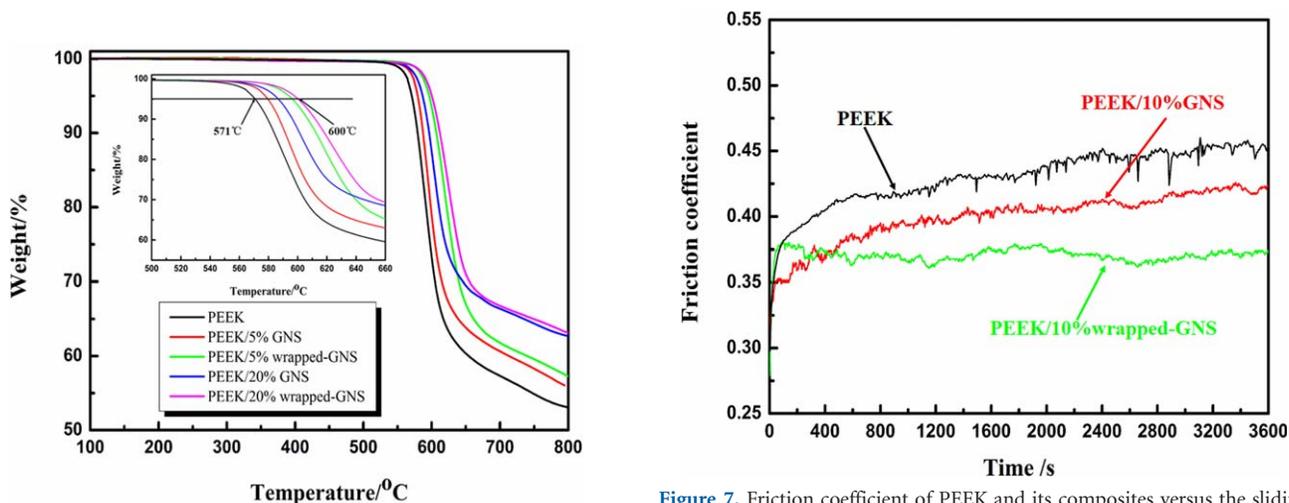


Figure 6. TGA curves of PEEK and its composites heated at 10°C/min under nitrogen. [Color figure can be viewed in the online issue, which is available at wileyonlinelibrary.com.]

Figure 7. Friction coefficient of PEEK and its composites versus the sliding time. Test conditions: applied load = 1 MPa and sliding velocity = 1 m/s. [Color figure can be viewed in the online issue, which is available at wileyonlinelibrary.com.]

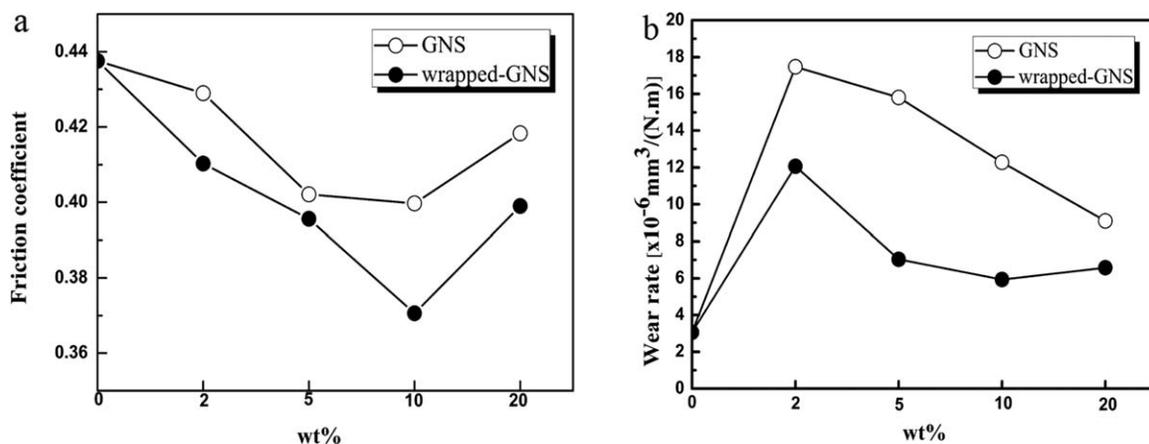


Figure 8. (a) Friction coefficient and (b) wear rate values of PEEK and its composites. Test conditions: applied load = 1 MP and sliding velocity = 1 m/s.

the PEEK/GNS composites was smoother and had a lot of small defects. Figure 9(e,f) shows the worn surface of the PEEK/wrapped GNS composites and shows their smoother

surface compared to those of the pure PEEK and PEEK/GNS composites; this was attributed to the enhanced dispersion and interfacial compatibility by the PES intermediate layer.

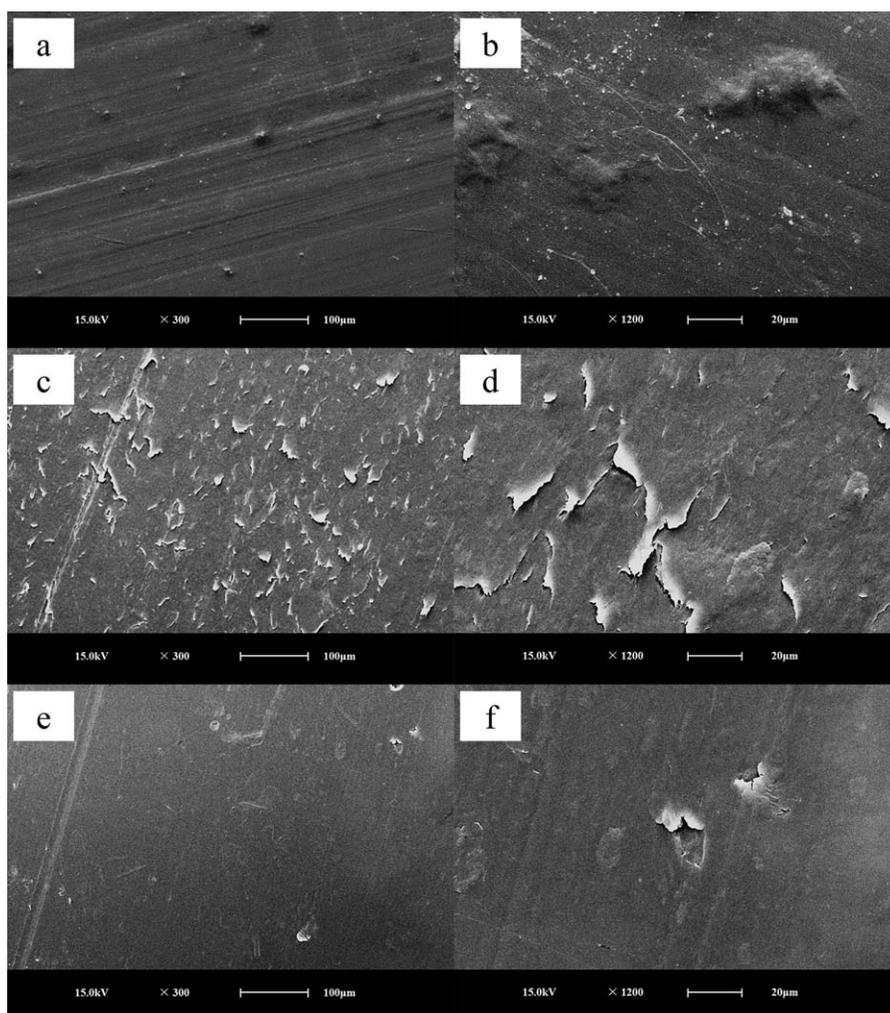


Figure 9. Worn surfaces of PEEK with (a) low and (b) high magnifications, GNS/PEEK composites at GNS proportions of 10 wt % with (c) low and (d) high magnifications, and wrapped GNS/PEEK composites at wrapped GNS proportions of 10 wt % with (e) low and (f) high magnifications.

CONCLUSIONS

PEEK/wrapped GNS composites were successfully obtained via a melt-blending route. Within such a system, PES was used as intermediate layer to not only eliminate GNS aggregation inside the PEEK matrix for homogeneous distribution inside the PEEK matrix but also enhance the interfacial adhesion between the PEEK and wrapped GNSs. Thus, an excellent tribological performance and low friction coefficient/wear rate were achieved; this makes our sample a potential metal replacement solution in applications such as seals, connectors, test sockets, and wire coatings. This is important to drive down vehicle costs and weights in the automotive industry.

REFERENCES

1. Rong, C.; Ma, G.; Zhang, S.; Song, L.; Chen, Z.; Wang, G.; Ajayan, P. M. *Compos. Sci. Technol.* **2010**, *70*, 380.
2. Cebe, P.; Hong, S. D. *Polymer* **1986**, *27*, 1183.
3. Talbott, M. F.; Springer, G. S.; Berglund, L. A. *J. Compos. Mater.* **1987**, *21*, 1056.
4. Sarasua, J. R.; Remiro, P. M.; Pouyet, J. *J. Mater. Sci.* **1995**, *30*, 3501.
5. Mens, J. W. M.; De Gee, A. W. *J. Wear* **1991**, *149*, 255.
6. Lu, Z. P.; Friedrich, K. *Wear* **1995**, *181*, 624.
7. Bijwe, J.; Sen, S.; Ghosh, A. *Wear* **2005**, *258*, 1536.
8. David, D. L.; Burris, W. G. *Wear* **2006**, *261*, 410.
9. Wang, J.; Zhang, R.; Xu, J.; Wu, C.; Chen, P. *Mater. Des.* **2013**, *47*, 667.
10. Marcon, A.; Melkote, S.; Kalaitzidou, K.; DeBra, D. *CIRP Ann.—Manuf. Technol.* **2010**, *59*, 141.
11. Alberts, M.; Kalaitzidou, K.; Melkote, S. *Int. J. Machine Tools Manuf.* **2009**, *49*, 966.
12. Wang, L.; Zhang, L.; Tian, M. *Wear* **2012**, *276*, 85.
13. Friedrich, K.; Zhang, Z.; Schlarb, A. K. *Compos. Sci. Technol.* **2005**, *65*, 2329.
14. Hale, W. F.; Farnham, A. G.; Johnson, R. N.; Cledinning, R. A. *J. Polym. Sci. Part A-1: Polym. Chem.* **1967**, *5*, 2399.
15. Rao, V. L.; Sabeena, P. U.; Rao, M. R.; Ninan, K. N. *J. Appl. Polym. Sci.* **1999**, *73*, 2113.
16. Sur, G. S.; Sun, H. L.; Lyu, S. G.; Mark, J. E. *Polymer* **2001**, *42*, 9783.
17. Li, X. G.; Shao, H. T.; Bai, H.; Huang, M. R.; Zhang, W. *J. Appl. Polym. Sci.* **2003**, *90*, 3631.
18. Ramanujam, B. T. S.; Mahale, R. Y.; Radhakrishnan, S. *Compos. Sci. Technol.* **2010**, *70*, 2111.
19. Wang, F. J.; Li, W.; Xue, M. S.; Yao, J. P.; Lu, J. S. *Compos. B* **2011**, *42*, 87.
20. Wang, H.; Wang, G.; Li, W.; Wang, Q.; Wei, W.; Jiang, Z.; Zhang, S. *J. Mater. Chem.* **2012**, *22*, 21232.
21. Milani, M. A.; Quijada, R.; Basso, N. R.; Graebin, A. P.; Galland, G. B. *J. Polym. Sci. Part A: Polym. Chem.* **2012**, *50*, 3598.
22. Gopakumar, T. G.; Page, D. J. Y. S. *Polym. Eng. Sci.* **2004**, *44*, 1162.
23. Wang, Q.; Jiang, W.; Guan, S.; Zhang, Y. *J. Inorg. Organomet. Polym. Mater.* **2013**, *23*, 743.
24. Jiang, W.; Liu, Y.; Wang, J.; Wang, Q.; Zhang, Y.; Guan, S. *J. Appl. Polym. Sci.*, DOI: 10.1002/app.40028.
25. Nielsen, L. E. *Mechanical Properties of Polymers and Composites*; Marcel Dekker: New York, **1974**; Vol. 1.
26. Berlin, A. A.; Volfson, S. A.; Enikolopian, N. S.; Negmatov, S. S. *Principles of Polymer Composites*; Springer: Berlin, **1986**; Vol. 10, p 124.
27. Xie, G. Y.; Zhuang, G. S.; Sui, G. X.; Yang, R. *Wear* **2010**, *268*, 424.
28. Wang, L.; Zhang, L.; Tian, M. *Wear* **2012**, *276*, 85.